EURASIP Journal on Applied Signal Processing 2005:14, 2341–2358

A Multitarget Tracking Video System Based on Fuzzy and Neuro-Fuzzy Techniques

Jesús García

Departamento de Informática, Universidad Carlos III de Madrid, Avda de la Universidad Carlos III 22, Colmenarejo 28270, Spain
Email: jgherrer@inf.uc3m.es

José M. Molina

Departamento de Informática, Universidad Carlos III de Madrid, Avda de la Universidad Carlos III 22, Colmenarejo 28270, Spain
Email: molina@ia.uc3m.es

Juan A. Besada

E.T.S.I. Telecomunicación, Universidad Politécnica de Madrid, Ciudad Universitaria s/n, Madrid 28040, Spain
Email: besada@grpss.ssr.upm.es

Javier I. Portillo

E.T.S.I. Telecomunicación, Universidad Politécnica de Madrid, Ciudad Universitaria s/n, Madrid 28040, Spain
Email: javierp@grpss.ssr.upm.es

Received 19 December 2003; Revised 23 December 2004

Automatic surveillance of airport surface is one of the core components of advanced surface movement, guidance, and control systems (A-SMGCS). This function is in charge of the automatic detection, identification, and tracking of all interesting targets (aircraft and relevant ground vehicles) in the airport movement area. This paper presents a novel approach for object tracking based on sequences of video images. A fuzzy system has been developed to ponder update decisions both for the trajectories and shapes estimated for targets from the image regions extracted in the images. The advantages of this approach are robustness, flexibility in the design to adapt to different situations, and efficiency for operation in real time, avoiding combinatorial enumeration. Results obtained in representative ground operations show the system capabilities to solve complex scenarios and improve tracking accuracy. Finally, an automatic procedure, based on neuro-fuzzy techniques, has been applied in order to obtain a set of rules from representative examples. Validation of learned system shows the capability to learn the suitable tracker decisions.

Keywords and phrases: fuzzy-knowledge-based system, neuro-fuzzy learning, video image tracking, data association.

1. INTRODUCTION

In airport areas, advanced surface movement, guidance, and control systems (A-SMGCS) [10] are conceived as new procedures and technologies to support ground traffic management, increasing both safety and efficiency of traffic flow in complex, high-density airport ground scenarios. One of the core functions within A-SMGCS is surveillance, in charge of the automatic detection and tracking of all relevant targets located in the airport movement area (runways, taxiways, and apron areas). These targets moving in the airport are generally commercial aviation aircraft and surface vehicles, such as fuel trucks, luggage convoys, cars, and so forth. A-SMGCS processes data from different types of sensors to monitor all ground traffic providing controllers with a periodically updated synthetic image containing all interesting traffic state on the airport surface.

In this paper we will focus on tracking aspects when the data to be processed are provided by cameras. They act as noncooperative sensors, so not requiring additional equipment on-board for targets to be controlled. Cameras can be configured as a set of local installations with high resolution of the images produced, allowing tracking in dense airport areas such as inner taxiways and apron. The general architecture and main blocks integrated in the video surveillance system were described in [3]. Basically, the system follows a distributed structure with a local processor operating on the image sequences provided by each camera. Each processor calculates target trajectories (local tracks) in the projected camera plane by performing two steps. First, moving targets are detected against their local background to generate detected pixels, connecting them later to form image regions referred to as blobs. Blobs are defined with their spatial borders, generally a rectangular box, centroid location, and area. Then, the tracker must distinguish all targets in the scene and track their motion, applying association and filtering processes to blobs extracted from the processed images.

The traditional association systems use, together with motion estimation, target position (represented by centroids) extracted from sensor data. Conventional nearest neighbor systems [5] deal with the assignment between plots and tracks as if minimizing a global cost function. This function is computed based on the distance between plots and predicted tracks (residuals) and known statistical models for sensor errors. Bayesian extensions of NN, such as multiple hypothesis tracking (MHT) [5] consider association decisions over several data scans to ensure track continuity under critical conditions such as presence of false alarms, maneuvers, or closely spaced targets. These types of hard-decision systems assume basic constraints of single plot updating each track, and no more than one track updated by the same plot, which are not applicable to the problem at hard.

A possible solution could be the removal of the one-to-one constraints and the enumeration of all possible grouping and assignment hypothesis with approaches similar to that suggested in [11]. However, these types of solutions could demand excessive computation load to process the frames in real time and it would not ensure solving some problems such as the assignation of corrupted blobs resulting from the mix of several target images. As alternative, an all-neighbors approach, similar to joint probabilistic data association [5] or PMHT [12], seems adequate to this problem, since all blobs potentially gated with each track are used to update it, requiring besides quite lower memory and computation than MHT approaches. Other approaches apply the expectation-maximization [8] clustering algorithm for estimating the unknown correspondence among blobs and tracks. The groups of cells representing each target are modelled as a mixture of Gaussian pdf's of unknown parameters, so a likelihood function for those parameters given the measurements are computed at the same time as the unknown correspondence. The application of EM algorithm transforms the hard assignment to a continuous problem, numerically solved with a “hill-climbing” approach. It has been previously applied to data association for computer vision applications [7], and for a probabilistic approach to MHT, PMHT [12].

Using a video surveillance system, an explicit representation of target shape and dimensions seems more adequate than a simple position to improve the association logic in order to select the set of updating blobs for each track. There are many approaches for video-based tracking systems based on regions in the computer vision literature, for instance, [23, 24]. Some proposals use in addition 3D models of interesting targets which are projected on camera plane, and then a correlation process allows model identification and extraction of parameters such as position or orientation [13, 16]. However, these systems require detailed 3D models of all interesting targets, which may be difficult in heterogeneous airport scenarios, and they could be computationally expensive in situations with a moderate number of targets.

The approach proposed here does not take advantage of any 3D information; it uses a generic 2D model based on moving regions to represent the targets. The central problem addressed is the correspondence between tracked objects and extracted regions making use of a spatial shape representation and a rule-based system. Besides, the rules also address the evolution of shape (it depends on the relative position of target with respect to camera plane), which is updated accordingly to the information received from the images sequence.

The updating scheme should be designed considering a number of factors to overcome all the specific problems and effects with video data, in order to guarantee the stability of the tracking output. There are no detailed models or analytical expressions to design this process, similar to JPDA [9] where there is full-detailed statistical model of sensor data. As an alternative, this paper presents a representation of knowledge in order to enhance the tracking performance. An analysis of continuity performance with different strategies, depending on numeric heuristics describing the possible situations to solve, may potentially provide robust rules to take appropriate association decisions [11].

The proposed algorithm estimates a correlation level, assessing the confidence given to every blob for updating every track, with a number of rules derived from experimentation. Rules can be obtained by analysis of conventional tracking systems performance under different conditions, characterized with these heuristics values. The rules represent the suitable actions to take under a set of particular extreme conditions to guarantee track continuity. Fuzzy reasoning techniques [19, 28] may be adopted to reproduce the system behavior under these extreme conditions, and besides generate the proper output for all intermediate cases. One of the advantages of this soft approach is that it avoids combinatorial complexity, essential to real-time operation with moderate frame rates, since it removes enumeration of hypotheses, while it is flexible to include specific rules to deal with the most complex situations. The fuzzy system will compute for each blob potentially gating each track a weight to be considered in the track update, so that several blobs can contribute in final estimation.

Finally, learning techniques can be potentially exploited to automatically learn and tune the proposed rule system. A machine-learning procedure (neuro-fuzzy technique) has been applied in order to extract rules directly from examples, analyzing the capability to provide right decisions in different conditions.

The rest of paper is organized as follows. In the next section, the particular association problems in this type of application are summarized and taken as the objective of design. Section 3 presents the representation of target shape and the heuristics considered to describe the image characteristics. The fuzzy approach to evaluate the confidence levels used to update estimators describing targets shapes and motion

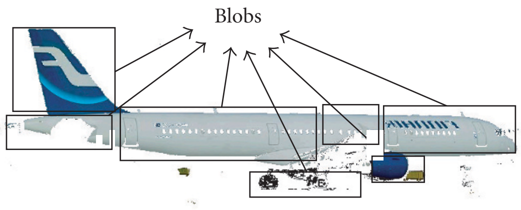

Figure 1: Blob-to-track association problem.

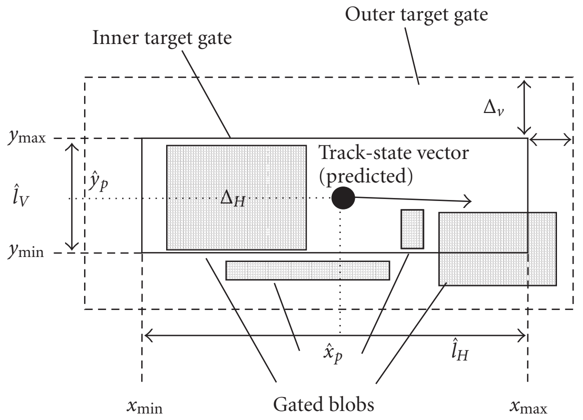

Figure 2: Target segmentation with estimated box.

parameters is presented in Section 4, including the learning approach based on a neuro-fuzzy technique. Section 5 is dedicated to evaluation, and the system output in several scenarios is analyzed indicating the response for complex situations with real image sequences of representative ground operations. The end of this section is related with the application of the learning method and the evaluation of the learned rules. Finally, some conclusions and future work are presented in Section 6.

2. THE MULTITARGET TRACKING PROBLEM IN VIDEO SURVEILLANCE SYSTEMS

As mentioned above, the design of a multitarget tracking system must address the data association logic [5], which is the focus of interest in this case of video data processing. Its design must take into account the characteristics and quality of data resulting from the detection subsystem. In this case, data are the blobs resulting from the detection subsystem applied on image sequences of airport surface scenes.

Figure 1 shows an example where a single target (an aircraft) is the source for five blobs separated from the background. When processing video output in dense airport areas, each available frame presents a set of blob-to-track multiassignment problems to be solved, where several (or none) blobs may be assigned to the same track and simultaneously several tracks could overlap and share common blobs.

So the association problem to solve is the decision of the most proper grouping of blobs and assignation to each track for each frame processed. The characteristics of data to be processed, blobs detected in image sequences of airport surface areas, have been taken into account to develop the image-based tracking system. Due to image irregularities, shadows, occlusions, and so forth, a first problem of imperfect image segmentation appears resulting in multiple blobs potentially generated for a single target. This splitting effect occurs with extraneous surface objects such as luggage convoys, or presence of irregular shadows, and especially when obstacles or other targets appear between the interest target and camera. So, blobs must be reconnected before track assignment and updating. This problem might be easily solved in single-target scenarios using a blob-grouping algorithm based on the blobs associated to the track in previous frames, defining a spatial gate for each track. However, when multiple targets move closely spaced, their image regions interact and overlap causing some targets to appear occluded by other targets or obstacles, so that some blobs can be shared by different tracks. So, a blob-to-track multiassignment problem has to be solved, where several blobs could be assigned to the same track and simultaneously several tracks could overlap and share common blobs. The key trade-off to be considered in the system performance can be summarized in the following two aspects, which represent conflicting requirements:

(1) it must group the different blobs representing a single target to avoid track-splitting effects. Grouping must adapt to gradual variations in targets sizes and shapes due to changes in distances and orientations of targets;

(2) when different targets approach one another, it should avoid mixing their close image regions since their tracks can be wrongly updated or even one of them discarded resulting in an erroneous single track including more than one target.

Besides, the case of no plot updating the track (track predicted) is also weighted and included to generate the final pseudomeasure to update the track. If more than one blob is within track gate, their centroids are combined after, using their areas as weighing factors to finally update the track.

Finally, a recursive filter is used to update both centroid position and velocity for each track from the sequence of assigned values, by means of a decoupled Kalman filter for each Cartesian coordinate, with a piecewise constant white acceleration model [5]. So, the association of blobs to tracks determines the evolution of tracks representing the targets. The logic included in the fuzzy system is mainly intended to keep tracks continuity in real conditions.

3. REPRESENTATION OF TARGETS SHAPES AND ASSOCIATION HEURISTICS

In the developed visual tracking system, track-state vectors with position and cinematic estimates (2D location and velocity referred to the camera plane) are complemented with attributes defining a spatial representation of target extension and shape. So, the predicted target contour is used to gate blobs extracted in next frame.

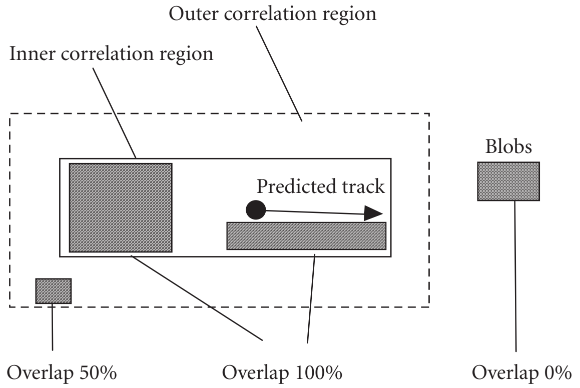

Figure 3: Overlapping degree heuristic.

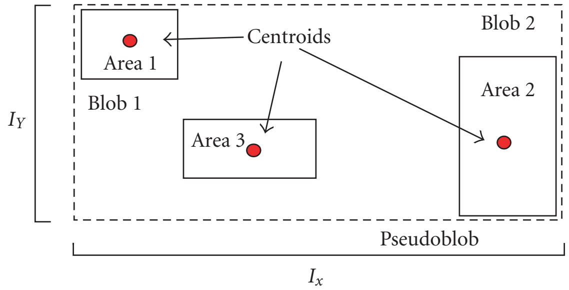

Figure 4: Group density after blob reconnection.

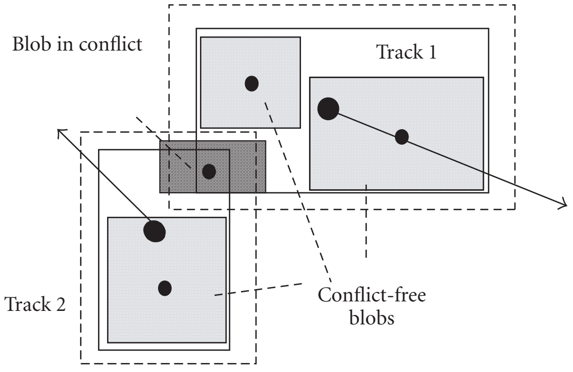

Figure 5: Blob in assignment conflict with two tracks.

For the sake of simplicity, a rectangular box has been used to represent the target, as indicated in Figure 2. Around the predicted position, $(\hat{x}_p, \hat{y}_p)$, a rectangular box is defined, $(x_{\min}, x_{\max}, y_{\min}, y_{\max})$, with the estimated target dimensions $(\hat{l}_H, \hat{l}_V)$. Then, an outer gate, computed with parameters Δ_H, Δ_V, is used to finally gate the potential blobs updating the track estimates.

This outer gate allows the system to track dynamic variations in target shape along the sequence for targets not perfectly matching the predictions due to variations in projected shape (changes of orientation, distance, etc.), or maneuvers. Besides, it avoids the initialization of tracks around existing ones, potential source of instabilities. The process of shape update with new information should reach a trade-off between the conflicting requirements presented in previous section: it must reconnect the different blobs representing a single target to avoid track-splitting effects and, when different targets approach one another, it should avoid grouping their image regions since their tracks could be wrongly updated. So, the shape must be dynamically updated with the information contained in blobs, but the changes must be smooth, avoiding instabilities in scenarios with closely spaced targets.

The final weight of gated blobs in the update phase should take into account the aspects mentioned before. Although there is not any closed expression doing that, similar to statistical residuals, some numeric heuristics, computed with simple geometrical analysis of blobs and predicted tracks, have shown to provide helpful indications to be considered. They can be used to asses the confidence given to each blob after it is included into a certain group, and also to assess confidence in predicted track. They were detailed in [11], and are summarized as follows.

(1) *Overlapping heuristic*: this component can be seen as a "soft gating," computed as the fraction of blob area contained within track-predicted region. Maximum value, 1, is given when blob is completely included within an inner track-predicted gate, and minimum, 0, when blob is out of an outer track region (see Figure 3). Both regions for each track allow adaptive grouping for targets not perfectly matching predictions due to variations in projected shape (changes of orientation, distance, etc.), or maneuvers.

(2) *Group density and distance to track*: this heuristic, ρ, evaluates the ratio between areas of detected regions and nondetected zones (holes) in the box enclosing the finally reconnected pseudoblob (see Figure 4). $\rho = \sum_i \text{Area}_i/(l_x l_y)$. So, in the case that the blobs grouped are very scattered, a low value of ρ will indicate that different targets probably have originated them.

To do that, a criterion based in the distance to track is used to finally compute this heuristic whose values fall from 1, when distance is zero, to ρ, for the most separated blobs, so that they would be practically discarded when density is low.

(3) *Conflict with other tracks*: this component evaluates the likelihood of blob being in conflict with other tracks. This problem appears when target trajectories are so close that track gates get overlapped and share the blob, as depicted in Figure 5.

Evaluation of blob conflict degree is completely equivalent to the first heuristic, overlapping, but computed with the other existing tracks. In the case that more than one track are in conflict, the maximum overlapping degree is selected.

(4) *Proximity to image borders*: finally, image borders are the areas where tracks are usually initialized, and so they are transient areas where tracks are not stabilized yet. This number evaluates if the blob is close to any of the four image borders.

These heuristics provide useful information to be considered when assessing the confidence that may be given to each blob before track update. Additionally, the predicted track may be also characterized with some heuristics, indicating the confidence given to the fact that this track represents motion of a real target. These track heuristics detect when it may be deviating from the real trajectory.

(i) *Number of missed updates*: it is the number of consecutive frames where no blob was included into track inner gate.

(ii) *Track detected area*: conversely to blob overlapping heuristic, it is the proportion of area, within predicted inner gate, filled with blobs detected in current frame.

(iii) *Proximity to image borders*: this value is equivalent to the one computed for blobs.

4. FUZZY SYSTEM FOR UPDATING TARGETS SHAPES

Heuristics defined above are the input to unknown relations computing the confidence levels both for blobs and predicted tracks in the update process. A rules system based on fuzzy logic has been developed in order to approximate these relations. The first step to build this system should be the selection of adequate descriptions of heuristics and rules relating them with the outputs: confidence levels for blobs and predictions. The inputs (heuristic values) are translated into linguistic variables. Using these concepts, for heuristic h_i, a linguistic variable Lh_i is introduced together with its set of values $\{lh_{i1}, lh_{i2}, \ldots, lh_{im_i}\}$, whose cardinality is m_i. Each term lh_{ij} in the set, labels a fuzzy subset in the universe of discourse H_i, with membership function $\mu_{lh_{ij}}(h_i)$. A fuzzy relational algorithm (FRA) will store the knowledge required to obtain the final confidence level, CONF, both for blobs and tracks involved in each decision. It is composed of a finite set of fuzzy conditional statements of the form IF $\{Lh_i \text{ is } lh_{ij}\}$ THEN $\{\text{LCONF is } l\alpha_k\}$, where LCONF is a linguistic variable representing blobs or track confidence levels, with a set of possible values $\{l\alpha_1, \ldots, l\alpha_n\}$. The Mamdani implication [17] has been chosen. Finally, α is the defuzzification of LCONF, and CONF represents its numerical domain (universe of discourse of LCONF). The adopted defuzzification process on LCONF will be a modified version of the center of gravity procedure [29].

Target's estimated shape will vary very smoothly, accordingly to confidence levels of gated blobs. The estimated position (measured centroid to update track vector) will depend both on these blobs confidence levels, α_{bi}, and on predicted track confidence, α_p, in order to avoid losing tracks when they deviate from real trajectory. So, estimated shape (dimensions of box) is the most constrained feature, remaining "locked" while the blobs confidence levels are not high enough, while estimated position (where the bounding box is located) will be a trade-off between confidence levels estimated both for blobs and tracks.

With the rectangular simplification considered, only two shape parameters are estimated: length, width $(\hat{l}_H, \hat{l}_V)$. If we consider horizontal coordinate, the two gated blobs with the minimum and maximum extremes for coordinate x, $(x_{b\min}, x_{b\max})$ are taken into account. Denoting their associated confidence levels, computed by fuzzy system, as α_{1H}, α_{2H}, the minimum and maximum values are obtained: $\alpha_{\min H} = \min[\alpha_{1H}, \alpha_{2H}]$; $\alpha_{\max H} = \max[\alpha_{1H}, \alpha_{2H}]$.

First, the target horizontal length is updated considering the minimum blob confidence value, $\alpha_{\min H}$:

$$\hat{l}_H[k] = \alpha_{\min H}(x_{b\max} - x_{b\min}) + (1 - \alpha_{\min H})\hat{l}_H[k-1]. \tag{1}$$

So, the estimated target length will be modified only in the case where both blobs have enough confidence. Then, the estimated target bounds (location of box) are updated from the blob with the highest confidence, $\alpha_{\max H}$, considering also the value for track confidence, α_p. It is required that α_p reaches a minimum threshold, T_p, to weight the track prediction with the blob having highest confidence. In other case, track prediction is discarded, and box is positioned aligned with the best blob, in order to avoid track lost when deviation between predictions and detected regions increases. For instance, if left-hand side blob defining value $x_{b\min}$ had the highest confidence, the estimated target bounds would be updated as follows.

(i) $\alpha_p > T_p$:

$$\begin{aligned}\hat{x}_{\min}[k] &= \alpha_{\max H} x_{b\min} \\ &\quad + (1 - \alpha_{\max H})(\hat{x}_{\min}[k-1] + \hat{v}_x[k-1]T), \\ \hat{x}_{\max}[k] &= \hat{x}_{\min}[k] + \hat{l}_H[k].\end{aligned} \tag{2}$$

(ii) $\alpha_p < T_p$:

$$\begin{aligned}\hat{x}_{\min}[k] &= x_{b\min}, \\ \hat{x}_{\max}[k] &= \hat{x}_{\min}[k] + \hat{l}_H[k].\end{aligned} \tag{3}$$

$(\hat{x}_{\min}[k-1], \hat{x}_{\max}[k-1])$ are the horizontal bounds in last update, $\hat{v}_x[k-1]$ the horizontal velocity estimated by tracking filter, $\hat{l}_H[k]$ the value computed in (1), and T the time elapsed. T_p is the threshold on track confidence. Similar considerations are made for the other possible case (right-hand blob) and for the vertical dimension update.

Figure 6 shows an example of track shape update with two targets overlapping, and performing maneuvers (track 1 represents a target accelerating and track 2 decelerating). Due to the conflicting blob, dimensions of both tracks remain locked in this frame, but bounds are computed to conform to the conflict-free blobs (with high confidence levels for association). So, the biases produced by maneuvers are corrected.

Finally, the measured target centroid used to update the estimated track vector is extracted from the set of blobs gated in the updated track contour, after applying the logic explained above to generate target bounds. To do that, only the portion of blobs within the track box are considered, and they are weighted with their areas, $x_a = \sum_i x_i A_i$, as indicated in Figure 7.

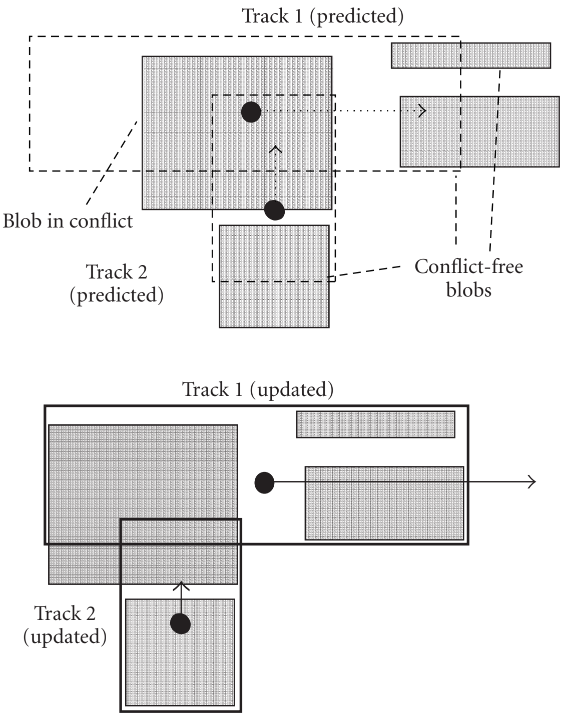

Figure 6: Shape update with conflicts and maneuvers.

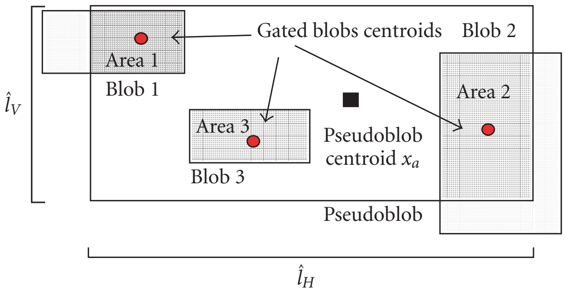

Figure 7: Centroid computation.

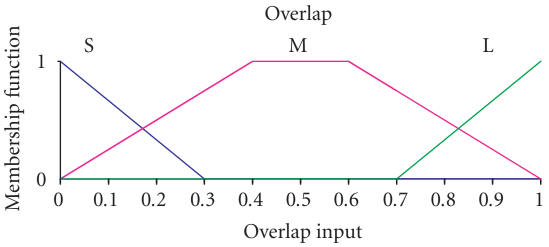

Figure 8: Membership function for overlap input.

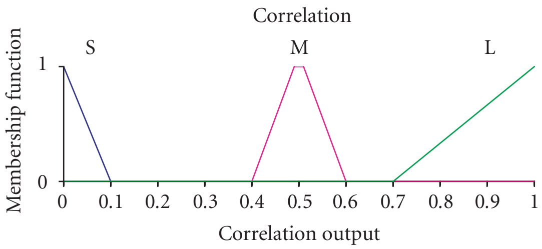

Figure 9: Membership function for blob correlation output.

The first implemented system had the seven inputs mentioned (overlap, density, conflict, border, track misses, track overlap, and track border) and two outputs, correlation level for blob,α_b, and track weight, α_p. Each linguistic variable was defined with three fuzzy sets: small (S), medium (M), and large (L). The membership function for them is indicated in Figure 8, common for all inputs, and Figure 9, for output α_b.

The rules were the following:

(i) overlap is small => correlation is small,
(ii) density is small => correlation is small,
(iii) conflict is large => correlation is small,
(iv) conflict is medium => correlation is small,
(v) (overlap is medium), (density is medium), and (conflict is small) => correlation is medium,
(vi) (overlap is medium), (density is large), and (conflict is small) => correlation is medium,
(vii) (overlap is large), (density is medium), and (conflict is small) => correlation is medium,
(viii) (overlap is large), (density is large), and (conflict is small) => correlation is large,
(ix) border is large => correlation is large.

This first system was manually set by analysis of tracking performance. Next, a data analysis was performed to automatically tune the fuzzy sets and rules, as indicated next.

4.1. Rule extraction using neuro-fuzzy techniques

An automatic learning procedure could be applied as an alternative to the manual derivation of the fuzzy rules from the expert knowledge, or to tune the labels' membership functions of linguistic variables used to represent the knowledge. Although many proposals have been developed based on neural networks [6] or in genetic algorithms [18], the fuzzy systems with learning techniques based on neural networks show mathematical consistence and have been applied profusely in many applications [14].

The techniques based on neural networks are named neuro-fuzzy systems and they are usually represented as a multilayer feedforward neural network [27]. A neuro-fuzzy system is a fuzzy system that is trained by a learning algorithm, usually related with neural network training methods. The learning process may be purely data driven or combined with a previous-knowledge-based system. In any case, the resulting neuro-fuzzy system will be interpreted as a system of fuzzy rules, so the learning procedure takes the semantic properties of the underlying fuzzy system into account (e.g., with constraints on the possible modifications of systems parameters).

Two approaches of neuro-fuzzy systems exist. The first type uses differentiable operators in the fuzzy system to apply gradient descent procedures. These systems, such as ANFIS or GARIC, generate fuzzy systems that are not easy to interpret. The ANFIS model by Jang [15] implements a Sugeno-like fuzzy system [26] in a network structure, and applies a mixture of backpropagation and least-mean-square procedure to train the system. The GARIC model [2] uses a special "soft minimum" function which is differentiable.

The second type of neuro-fuzzy system uses max-min operators and the learning procedure is heuristic, these systems are easy to interpret as the systems developed by Nauck and Kruse: NEFCLAS [20] and NEFCON [21]. The neuro-fuzzy system developed by Nauck and Kruse learns a fuzzy system in several steps. In the first place, it builds the fuzzy rule base using a labeled data set and a fuzzy classifier. Each fuzzy rule is a multidimensional fuzzy set covering a hyper-box in the data space. The membership degree of a cluster is the degree in which an individual pattern belongs to the cluster. The second step, starting with the learned rules (learned clusters), is the refinement of the membership functions to adjust the membership degree to the data set. This algorithm depends on the shape of the membership function (in the available software NECFLASS there are triangles, trapezoids, and bell-shaped functions). Finally, the last step is used to prune the fuzzy rule base. The pruning algorithm reduces the number of rules selecting the best rules and deleting the redundant ones.

The idea of the learning algorithm, see [22], is to create a rule base first and then to refine it by modifying the initially given membership functions (usually fuzzy partitions of input and output variables). The rule base is created by finding for each pattern in the training set a rule that best classifies it. If a rule with an identical antecedent is not already in the rule base, it will be added. The learning algorithm of the membership functions uses the output error that tells whether the degree of fulfillment of a rule has to be higher or lower. This information is used to change the input fuzzy sets by shifting the membership functions and making their supports larger or smaller. There are defined different shapes for fuzzy memberships (triangles, bells, etc.), and all of them can be easily modified with parameters. Constraints are defined here for the learning procedure (fuzzy sets must not pass each other or that they must intersect at 0.5, etc.), in order to obtain an interpretable rule base. After the rule learning algorithm has terminated, the predefined fuzzy partitioning on both input variables defines a partitioning of the input space created by overlapping hyperboxes where each hyper-box is formed by the Cartesian product of the supports of the defined fuzzy sets (the number of sets is predefined). Each hyper-box represents the support of an n-dimensional fuzzy set which is the antecedent of a fuzzy rule.

The fuzzy sets are trained by a backpropagation-like algorithm, the error is propagated from the output units towards the input units and is used to change the membership function parameters, but there is no gradient information involved. The adaptivity of an NEFCLASS system is restricted because of the initially given input fuzzy partitions, which define the form and maximal number of clusters, and by the constraints that do not admit certain changes in the fuzzy sets.

Finally, to interpret a fuzzy rule base it is important that there are as few rules as possible and that superfluous variables are not used in the rules. NEFCLASS defines pruning techniques to improve the rule base automatically. Besides, each of these pruning strategies can be interactively applied by the user with a graphical rule editor. Some of the strategies are related to rule evaluation (the rule learning procedure is invoked to keep only the best k rules) or to input deletion (the correlations of the input variables with the class information are computed in order to remove input variables with the worst correlation to the output).

In this paper, the fuzzy system for association used Mamdani implication [17] because the fuzzy system interpolates a generic function (the association function) without analytical expression. The Nauck/Kruse neuro-fuzzy approach was applied because it uses directly this type of implication and the method was developed for this type of fuzzy system. The goal of learning here was the suitable decision for each blob association to each track under different situations. The heuristic descriptors presented in Section 3 are used as input variables and the right decision, among three possibilities, is the available output, so it is a supervised learning. The details of learning process and the results about the capability of generalization from examples in this application are presented at the end of following section.

5. EXPERIMENTS AND PERFORMANCE RESULTS

This section presents some results about the performance of the developed video tracking system with real data from some sample scenarios. The evaluation of video tracking systems is an important aspect since it may require plenty of effort, especially when manual generation of ground truth is done. There are different approaches for performance assessing in the literature. The most direct is using manual mark-up of all samples, obtaining the "ideal" segmentation of all interesting targets from the background; there are available standard video sequences for test containing the ground truth, such as the PETS (performance evaluation of tracking systems) collections [23]. Other approaches make use of synthetic data or hybrid combinations of synthetic and real samples, such as [1, 4, 25].

This paper presents some demonstrative evaluation results, obtained with a direct supervision process, that illustrate the system's capability to cope with complex situations and include symbolic knowledge in the design. The only ground truth data generated were the labels for blob associations in some situations where learning was applied, leaving a more exhaustive evaluation and tuning for a future work. First, qualitative results are presented for continuity in some typical situations representing hard conditions of operation. Then, some quantitative results with accuracy are presented, comparing the fuzzy system with an ad-hoc system with hard-decisions for association, where the trajectories for comparison were approximated with least squares.

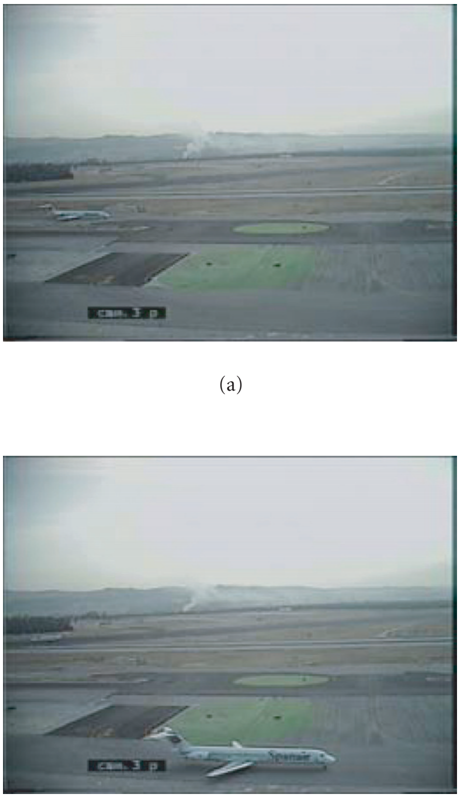

(a)

(b)

Figure 10: Single-target scenario 1. (a) $t = 15$ and (b) $t = 124$.

Finally, the section is closed presenting the automatic learning of association rules from data with a neuro-fuzzy model, and assessing the quality of learning in terms of generalization.

5.1. Continuity

First, the tracking output (estimated targets shape and cinematics) is presented for some representative scenarios, where the fuzzy association rules solved the most representative types of problems that can appear in the airport area. In all cases, blobs resulting from segmentation are always represented by dashed rectangles, with centroid location indicated with a circle. Tracks, predicted to the time instants of blobs detections, are represented by asterisks, vector velocity, and a solid rectangular target contour (inner correlation gate). Axis units are image pixels, and the time units are the frame numbers, with an average rate of 3 frames per second.

5.1.1. Scenario 1: single-target scenario

This situation has an aircraft detected, without other close targets, which performs a double turn to change the taxiway in which it is moving. In Figure 10, there are pictures for time instants before and after the maneuver. System output in six time instants is presented in Figure 11. The shape and area are continuously adapted to target dynamic evolution, and fragmented blobs are correctly reconnected, with maximum confidence levels.

5.1.2. Scenario 2: conflicts with two targets, no maneuvers

In this case, two aircrafts are moving in parallel taxiways and, due to the low depression angle, their images get mixed when they cross (Figure 12). System output in four representative time instants is presented in Figure 13. While targets are close, detection system extracts a single blob for two targets ($t = 47$, $t = 49$). The confidence level is lowered due to the conflict heuristic, and tracks shape and velocities are not affected during this interval. In $t = 50$, conflict degree is lower, confidence increases, and tracks are again updated with blobs.

5.1.3. Scenario 3: conflicts and occlusions

In this case, Figure 14 presents a situation where two effects, track conflicts and splits, due to occlusions, appear. A luggage convoy is partially occluded by an aircraft tail, and at the same time a high-speed van is moving in opposite direction. As shown in Figure 15, in time instants 113, 118, two blobs appear (indicated with discontinuous boxes), one as result of partial occlusion, and other in conflict with both tracks. Tracks shapes and locations are updated with blobs accordingly to confidence levels given basically by conflict degree, so the situation is correctly solved (tracks are displayed with continuous boxes and velocity vector superposed).

5.1.4. Scenario 4: conflicts and occlusions

In Figure 16, a multiple blob reconnection scenario is depicted. There is an aircraft moving from right to left, with occlusions due to a stopped bus and an aircraft located in front. As a consequence, multiple blobs representing different parts of aircraft and its shadow appear (see Figure 17, blobs are the discontinuous boxes with circles), and those are connected to update the aircraft track, without track-splitting effects. There are two continuous boxes representing the tracks for the aircraft and for an upper vehicle moving in a parallel inner taxiway, and the conflicts due to interactions when blobs are overlapped are correctly solved.

5.1.5. Scenario 5: conflicts and maneuvers

In this scenario, two aircrafts moving on inner taxiways between airport parking positions and maneuvering areas cross, as shown in Figure 18, and their images get mixed during 25 frames. Besides, both aircraft turn during the conflict interval changing their orientations. System output, with zoom in the interest targets, is shown in Figure 19 for four interest time instants. We can notice that the extracted blobs

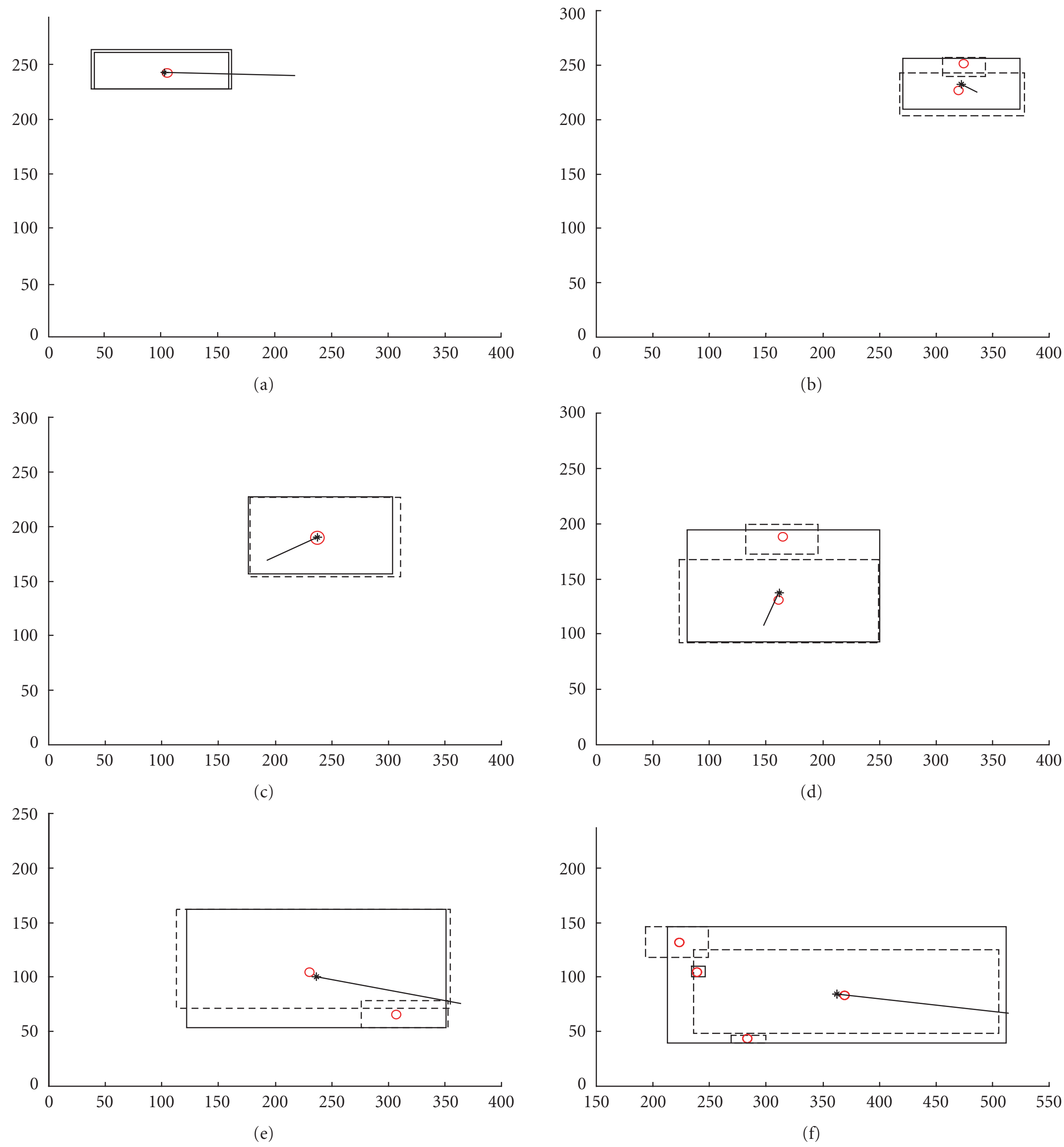

Figure 11: Shape evolution with single-target scenario 1: (a) $t = 15$, (b) $t = 50$, (c) $t = 75$, (d) $t = 100$, (e) $t = 116$, and (f) $t = 124$.

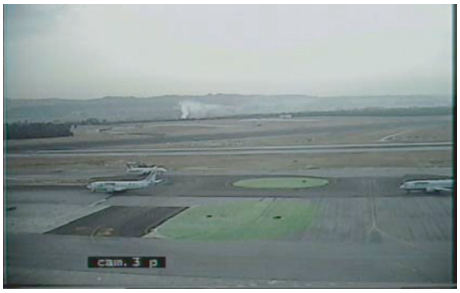

Figure 12: Constant-speed track conflict in scenario 2.

mix image regions from the two targets. In frame 90, due to conflict, a single discontinuous box melts the two aircrafts. The fuzzy system successfully avoids updating with the corrupted blobs and, as soon as targets separate (from frame 109 on) tracks (continuous boxes) are gradually updated to follow their respective trajectories.

5.1.6. *Scenario 6: conflicts and maneuvers*

Now, in the next example, three vehicles are moving on a road and approach one another until their images get overlapped, while at the same time one of them performs

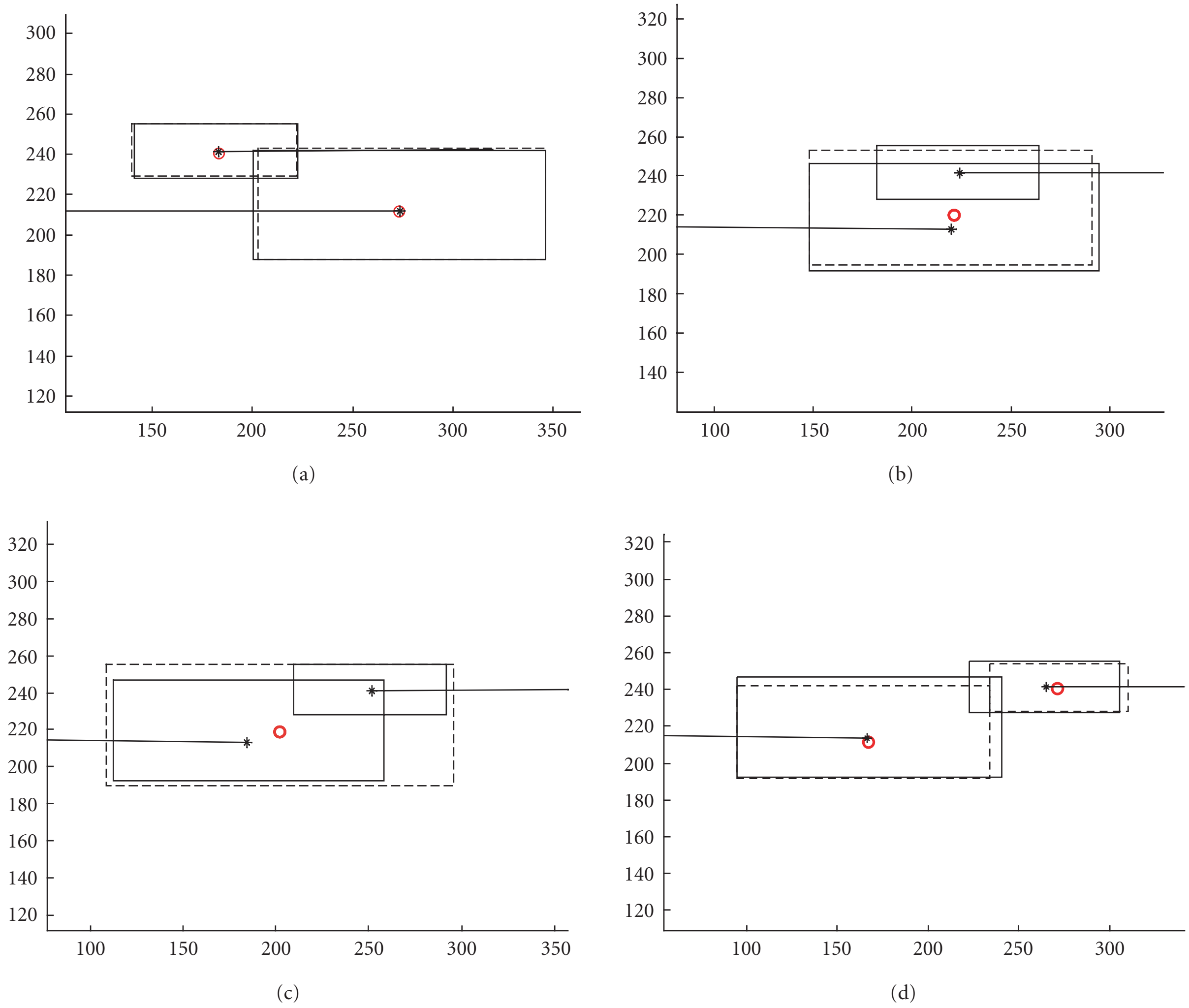

FIGURE 13: Shapes with a two-target conflict and constant velocity, scenario 2: (a) $t = 44$, (b) $t = 47$, (c) $t = 49$, and (d) $t = 50$.

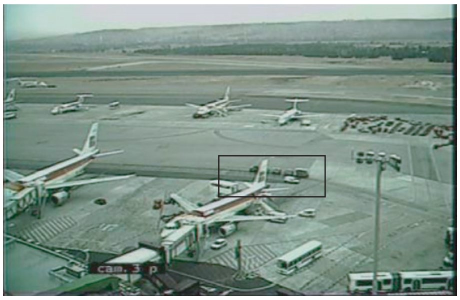

FIGURE 14: Track conflict and occlusion in scenario 3.

a deceleration maneuver. A van (white) and a vehicle move from left to right, and another vehicle is moving from right to left. As depicted in Figure 20, images from three vehicles overlap when the first vehicle moving from left to right stops in front of the aircraft. Figure 21 indicates some of the most important time instants, the blobs extracted by detector, and the tracks updated accordingly to the rules activated.

5.2. Accuracy

Here some comparative results about accuracy in two scenarios are presented, comparing the fuzzy system with an ad-hoc system with hard-decisions for association.

(i) Update with all blobs included in the gate if group density is higher than 0.7. Otherwise, remove the farthest blobs from the group.

(ii) If two or more tracks share any conflictive blobs, predict them without update.

Accuracy is defined by means of the root mean squared error (RMS) in the estimator for each coordinate. However, the analysis was performed over real data, without any reference trajectory available to compute the errors. To overcome this difficulty, a linear trajectory with uniform motion has been selected to reasonably estimate a least squares approximation from the track estimators as a reference to compute the errors.

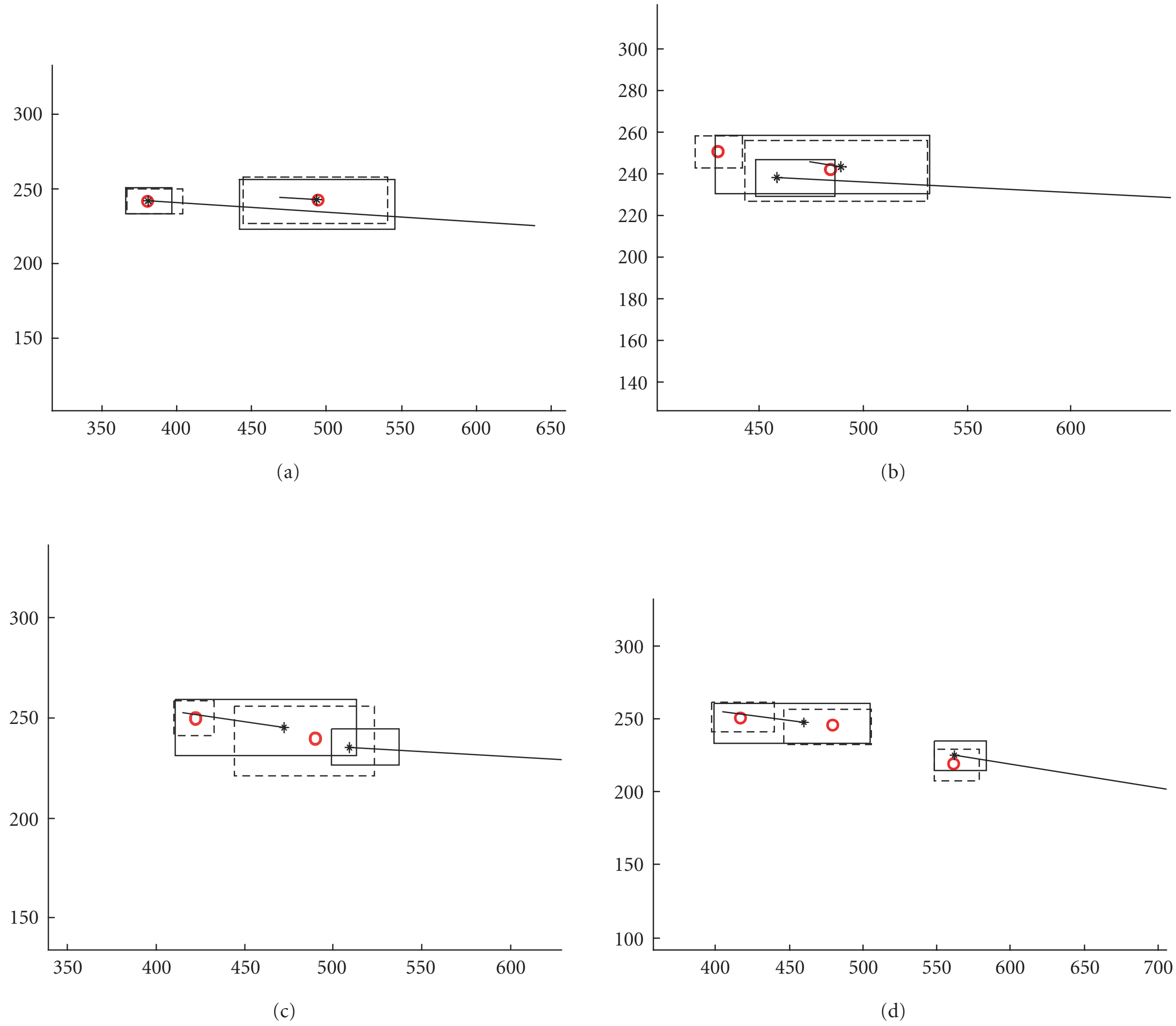

(a)

(b)

(c)

(d)

Figure 15: Output with reconnections and conflicts, scenario 3: (a) $t = 116$, (b) $t = 113$, (c) $t = 118$, and (d) $t = 120$.

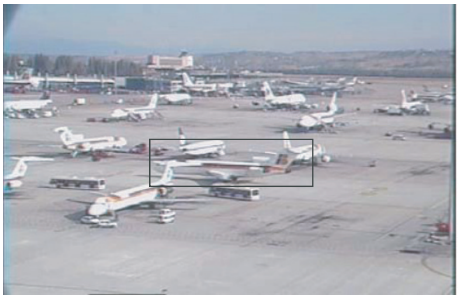

Figure 16: Target splitting in scenario 4.

Errors in scenario 4

First, the trajectory estimated for the aircraft in the 4th scenario above has been used to compare both systems. Target dimensions, available in the blobs extracted from images, normalize the errors and so they are expressed as fractions of target size in each coordinate (%). In that scenario there was an aircraft moving from right to left, with partial occlusions from a bus and an aircraft stopped in front. As a consequence, multiple blobs representing different parts of aircraft and its shadow appear, which are grouped to update the aircraft track (Id = 18), without splitting effects. Figure 22 shows the estimated trajectories (X, Y coordinates against processed frames) with fuzzy association (circles) and previous system (triangles), and an LS-approximated trajectory (dotted line). The normalized magnitude of error with respect to the straight line for X and Y coordinates is shown in Figures 23 and 24, respectively, comparing fuzzy and previous systems, which are represented by solid and dashed lines. RMS values, averaged along the time duration of trajectory are indicated too. As it can be seen, an improvement of 35%

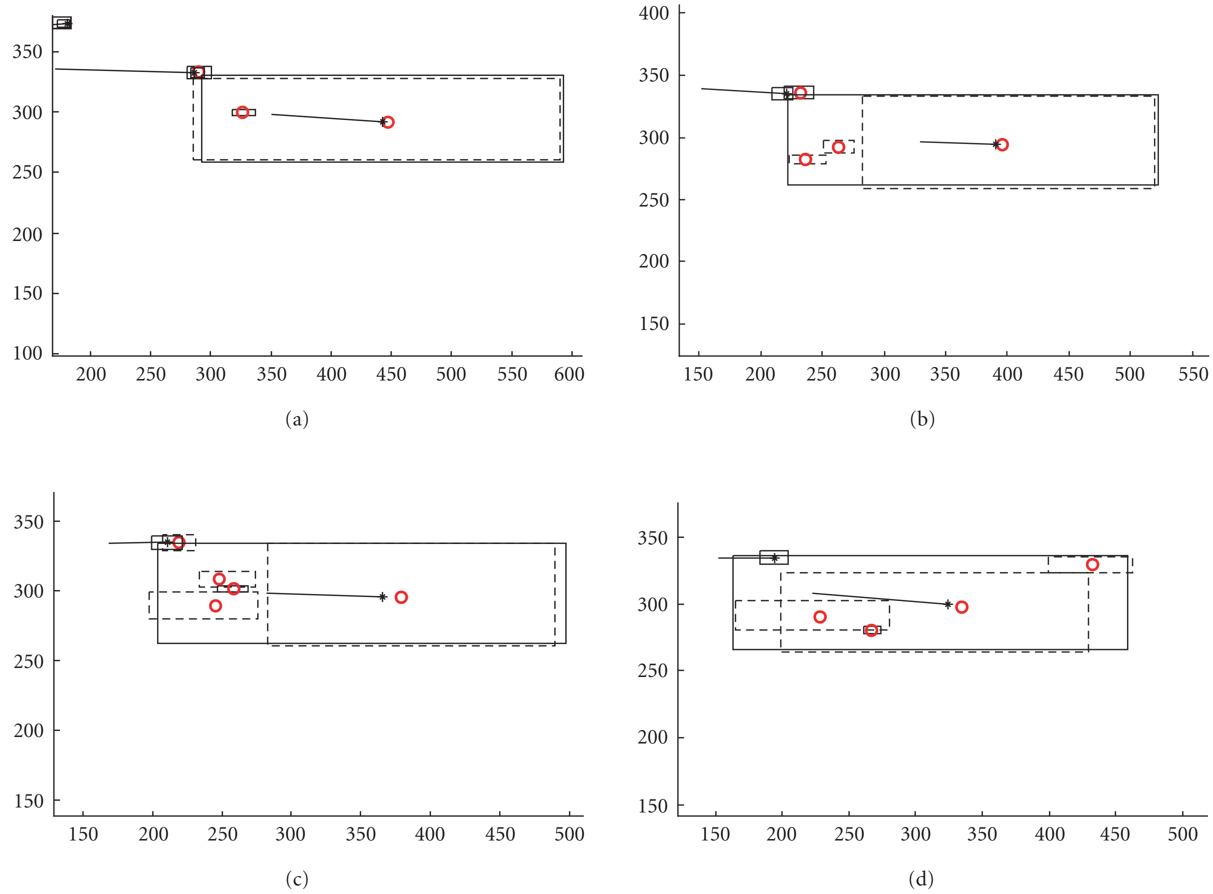

(a)

(b)

(c)

(d)

Figure 17: Blob reconnection with scenario 4: (a) $t = 89$, (b) $t = 96$, (c) $t = 99$, and (d) $t = 102$.

Figure 18: Low-density blob grouping and maneuvers in scenario 5.

in vertical accuracy appears with the new system, due to the fact that this track is more stable now, after integrating the fuzzy combination of blobs to be grouped.

Errors in scenario 5

In that scenario two aircrafts cross and their images get mixed with association conflicts for an interval of 25 frames (frames 90 to 113). In frame 95, where an aircraft is clearly occluded by another, fuzzy system successfully avoids update with corrupted blobs due to conflict, (frame 101), but as soon as targets separate (from frame 105), tracks are gradually updated to follow the trajectory. The output of both systems is displayed in Figure 25. The rigid system with extrapolation during conflicts clearly separates from real trajectory, due to maneuver during the conflict interval. This fact is illustrated in Figure 26, depicting the horizontal and vertical residuals with both systems (fuzzy with solid line, and previous one with dashed). In this case with maneuver it is not applicable using a linear approximation of trajectory, and so the residuals (difference between blobs centroids and track predictions) have been shown for evaluation.

5.3. Rules extraction with neuro-fuzzy techniques

Finally, here we present some results of automatic learning after applying the Nauck/Kruse neuro-fuzzy approach, described in Section 4.1, to learn rules from data. Three scenarios were selected from the set presented in Section 5.1 considering representative situations such as image splitting in segmentation, occlusions, and overlapping in order to get a robust system able to attain acceptable behavior in the general case. The three possible outputs considered for blob confidence regarding track parameters update were *discard, low,*

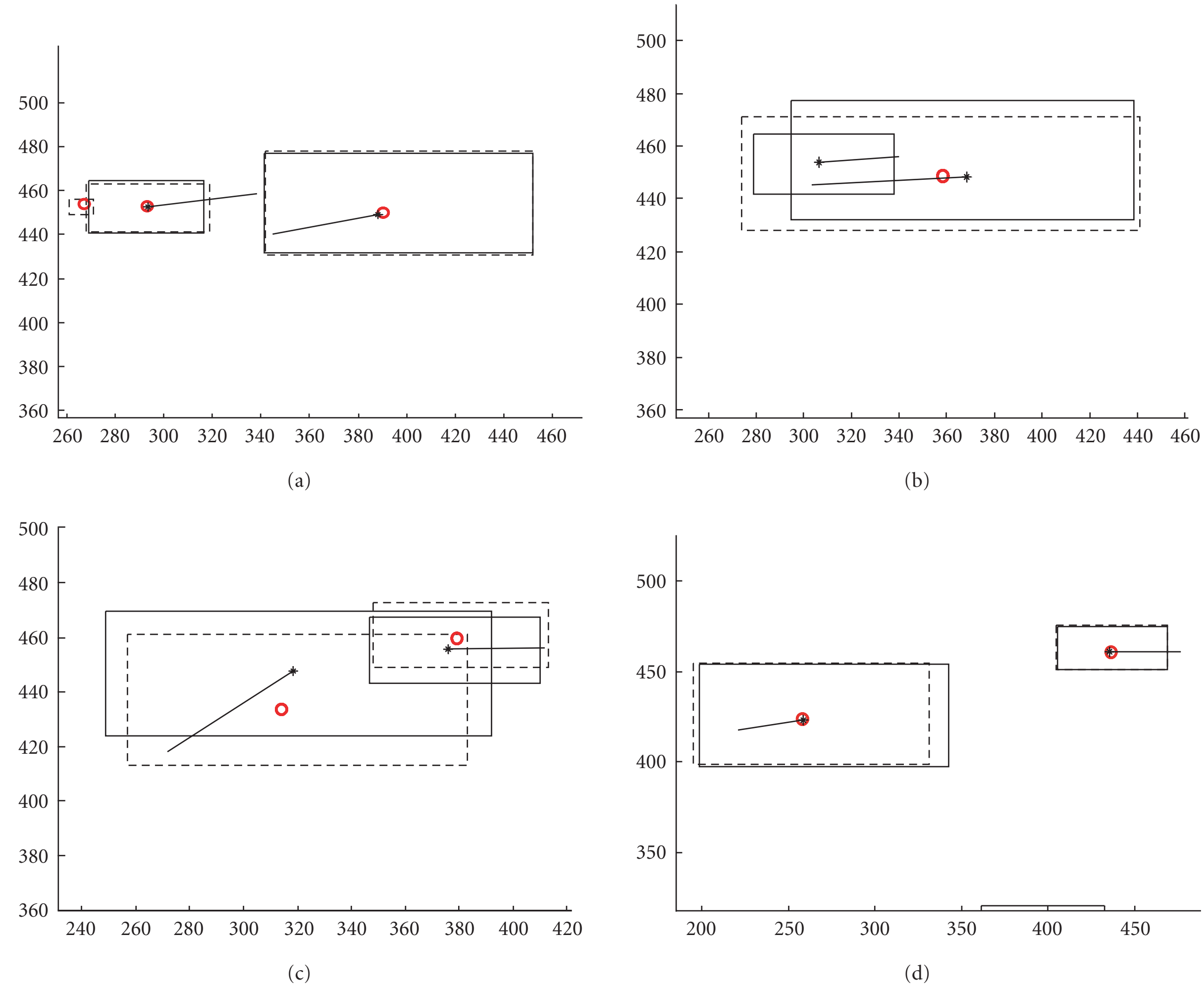

(a)

(b)

(c)

(d)

Figure 19: Shape evolution with scenario 5: (a) $t = 86$, (b) $t = 90$, (c) $t = 109$, and (d) $t = 118$.

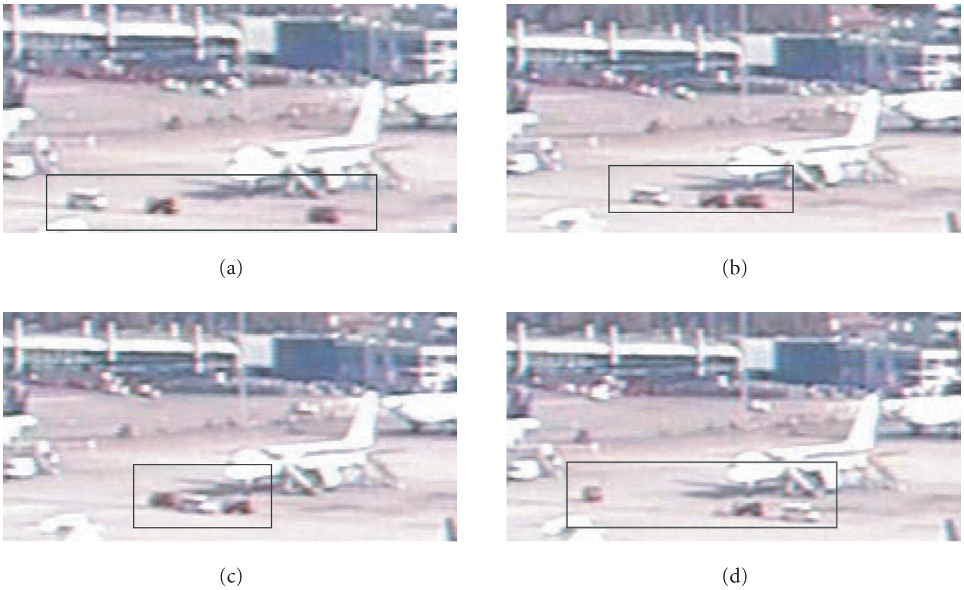

(a)

(b)

(c)

(d)

Figure 20: Blob reconnection and occlusions with scenario 6: (a) $t = 29$, (b) $t = 35$, (c) $t = 42$, and (d) $t = 55$.

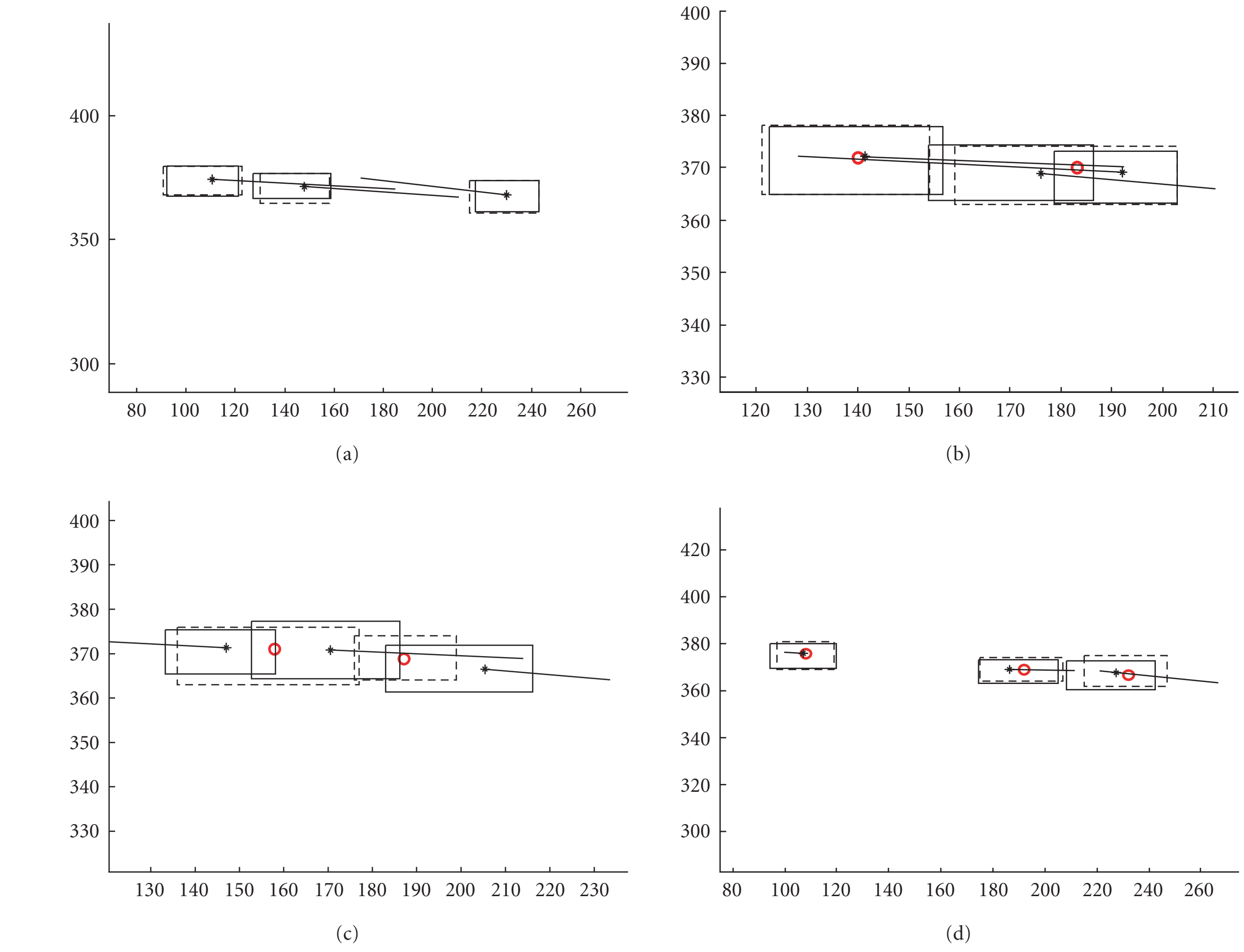

(a)

(b)

(c)

(d)

Figure 21: Tracker output in scenario 6: (a) $t = 29$, (b) $t = 35$, (c) $t = 42$, and (d) $t = 55$.

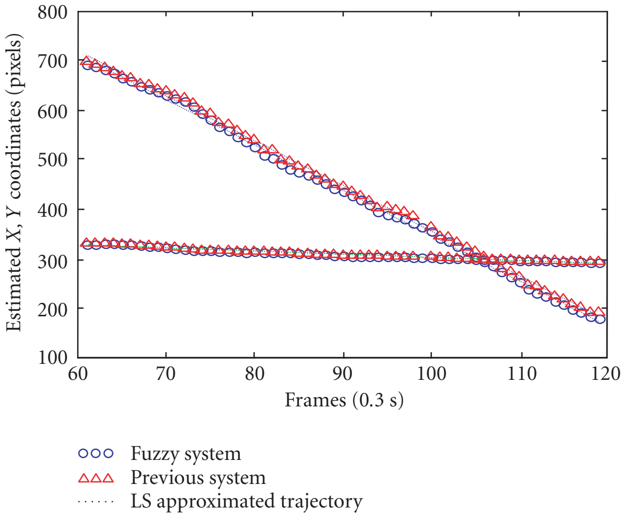

Figure 22: Estimated and approximated trajectories for track 18.

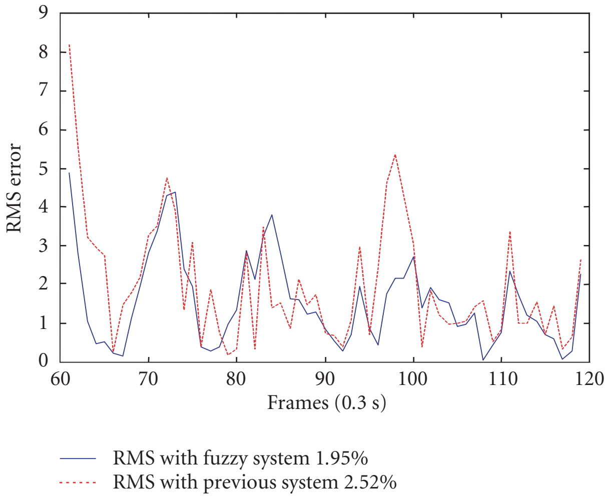

Figure 23: Horizontal error with respect to straight line.

high. So, for each detected blob located around the target bounds (predicted by the tracking system), the three possible decisions were as follows: accept the blob and update the estimated track parameters (high), if the blob information

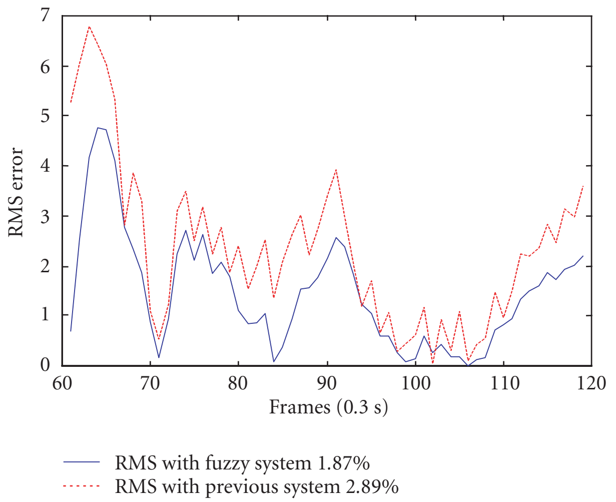

FIGURE 24: Vertical error with respect to straight line.

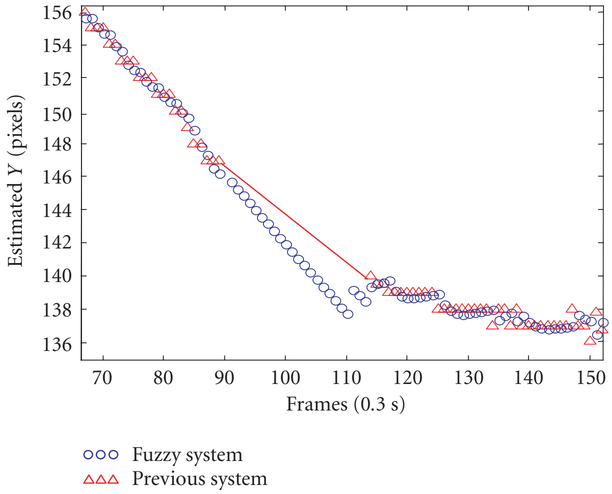

FIGURE 25: Estimated *Y* coordinate with both systems in scenario 5.

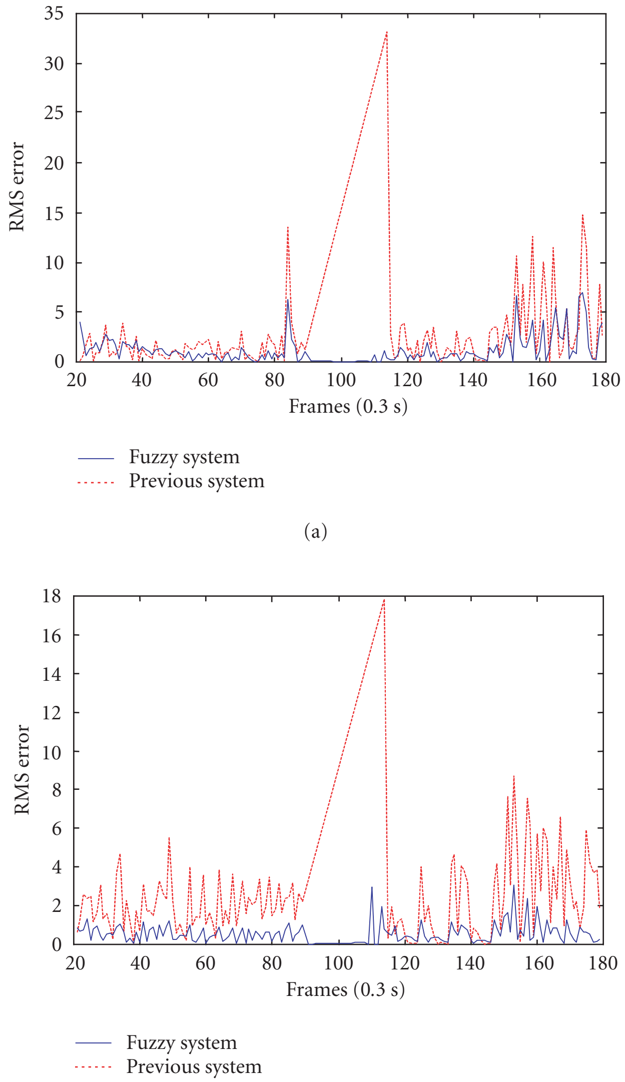

(a)

(b)

FIGURE 26: Residuals of both tracking systems in scenario 5: (a) horizontal residual (%) and (b) vertical residual (%).

is reliable and only referred to the represented target; discard the blob (discard), if it clearly comes from a different source; or partially update the track (low), when the blob has information about target but it is corrupted by effects such as occlusion or overlapping. The learning process then obtained a “synthetic” fuzzy system connecting these labels with the heuristics variables describing different situations. The three selected scenarios used to do that were the following.

(i) Scenario 2. Pairs of aircraft moving in parallel taxiways, with their images getting overlapped when they cross. The confidence level of blobs in such situations must be lowered to avoid degradation of estimated shape and kinematics of targets.

(ii) Scenario 4. Multiple blob reconnections. An aircraft is moving behind stopped vehicles and aircraft, which occlude it while other vehicles move in close parallel roads. Multiple blobs representing different parts of aircraft and its shadow appear. These blobs must be grouped to update the aircraft track, avoiding splitting effects. Besides, images from other vehicles must be kept separated guaranteeing track continuity for all targets.

(iii) Scenario 6. Three vehicles were moving on a road, approaching one another until their images overlap, while at the same time one of them performs a deceleration maneuver.

For each frame in these scenarios, the blobs and tracks were used to compute the heuristics, while the label describing the confidence category of blob (ground truth) was manually assigned from direct observation. The set of rules generated with all available data (around 250 frames, with 700 instances composed of 6 attributes and output), and using bell-shaped sets appears in Figure 27.

(i) If overlap T is large, density is medium, proximity is large, conflict is small, border is small, and overlap I is large, then high.
(ii) If overlap T is large, density is large, proximity is large, conflict is small, border is small, and overlap I is large, then high.
(iii) If overlap T is large, density is medium, proximity is large, conflict is small, border is medium, and overlap I is large, then high.
(iv) If overlap T is large, density is large, proximity is large, conflict is small, border is medium, and overlap I is large, then high.
(v) If overlap T is small, density is large, proximity is large, conflict is large, border is small, and overlap I is large, then discard.
(vi) If overlap T is small, density is medium, proximity is medium, conflict is medium, border is small, and overlap I is large, then discard.
(vii) If overlap T is small, density is medium, proximity is medium, conflict is large, border is medium, and overlap I is large, then discard.
(viii) If overlap T is small, density is medium, proximity is medium, conflict is large, border is small, and overlap I is large, then discard.

Figure 27: Rules automatically obtained.

Table 1: Accuracy of rules generated with different subsets of data.

	Test										
Training	S2 (22–43)	S2 (44–52)	S2 (53–88)	S4 (61–67)	S4 (72–137)	S4 (115–120)	S6 (40–63)	S6 (64–85)	S6 (86–111)	S6 (112–136)	All
S2 (22–43)	—	36.7	89.5	33.3	91.6	28	88.2	48.4	46.2	73.8	61.9
	—	43.3	94.7	53.3	99	44	94.1	60.5	65.1	100	76
S2 (44–52)	100	—	94.7	63.3	92.6	56	88.2	68.6	63.9	73.8	76.2
	93.5	—	81.6	63.3	74.7	64	79.4	67.7	60.3	70.2	70.2
S2 (53–88)	100	83.3	—	73.3	92.6	68	91.2	76.6	69.2	76.2	78.8
	100	86.7	—	86.7	100	84	94.1	96.8	94.7	100	95.7
S4 (61–67)	100	83.3	94.7	—	94.7	56	91.2	74.2	70.4	77.4	80.7
	96.8	90	96.1	—	84.2	80	82.4	67.7	74.6	96.4	81.2
S4 (72–137)	100	43.3	89.5	33.3	—	28	88.2	50	50.3	94.1	63.9
	100	43.3	94.7	53.3	—	44	94.1	60.5	65.1	100	73.7
S4 (115–120)	100	83.3	94.7	63.3	94.7	—	91.2	85.8	73.4	75	83.4
	100	86.7	96.1	76.7	92.6	—	91.2	95.1	89.4	73.8	89.6
S6 (40–63)	100	43.3	94.7	43.3	93.7	28	—	53.2	53.3	77.4	67.2
	100	43.3	94.7	53.3	99	44	—	60.5	65.1	100	76.2
S6 (64–85)	100	83.3	100	73.3	92.6	60	91.2	—	75.7	77.4	83.8
	100	86.7	100	86.7	96.8	84	94.1	—	91.7	85.7	92.5
S6 (86–111)	100	83.3	94.7	63.3	94.7	72	91.2	84.7	—	75	85.8
	100	86.7	100	86.7	99	76	94.1	96	—	100	95.9
S6 (112–136)	100	43.3	94.7	43.3	93.7	28	94.1	55.7	56.8	—	68.7
	100	43.3	94.7	53.3	99	44	94.1	60.5	65.1	—	73.9
Repres. 1	100	—	—	63.3	94.7	68	91.2	—	75.2	75	80.8
	100	—	—	76.7	100	84	97.1	—	94.1	97.6	94.9
Repres. 2	—	100	94.7	—	94.7	72	91.2	87.1	—	76.9	88.4
	—	86.7	100	—	96.8	84	97.1	97.6	—	83.3	93.8
All	—	—	—	—	—	—	—	—	—	—	84.1
	—	—	—	—	—	—	—	—	—	—	93.3
No. instances	31	30	76	30	95	25	34	124	169	85	699

We can compare these rules with the ones directly set to represent the "expert knowledge" in Section 4 and notice their similarities. As it can be seen, the most important attributes to classify blobs are again conflict degree and overlapping with track. Besides, in order to analyze the quality of the classification scheme and its capability to predict the tracker decisions, the whole data set was split in subsets for validation of learned rules. The three scenarios were divided into ten groups, depending on the characteristics of each sequence (segments without conflicts, segments with occlusions, with bad segmentations, etc.). These sets are summarized next.

(i) S2 (22–43), S2 (53–88): frames intervals of scenario 2 containing separated targets.
(ii) S2 (44–52): frames interval of scenario 2 containing conflicts with several interacting targets (crosses).
(iii) S4 (61–67), S4 (115–120): frames intervals of scenario 4 with no interactions.
(iv) S4 (72–137): frames interval of scenario 4 containing a target with reconnections due to background occlusions and interactions with a second target (vehicle).
(v) S6 (40–63), S4 (86–111): frames intervals of scenario 6 with interactions and occlusions.
(vi) S6 (64–85), S6 (112–136): frames interval of scenario 6 containing separated targets.
(vii) All: all frames available.

The training and evaluation process was performed with different scenarios to obtain the rate of instances correctly predicted in order to assess the ability to "generalize" suitable rules from sets of data representing different situations. The results are depicted in Table 1. Two types of fuzzy sets were selected to represent the concepts: triangular and bell-shaped, whose performances are indicated at the top and bottom, respectively, of each cell. From the results, the learning capability is generally better when bell-shaped functions are applied. The main diagonal is blank since the test was always performed with data different from training, in order to avoid over-fitting in the results. Final column has the mean performance for each training set applied to the rest of available data. The worst results were obtained when data from simple segments without problems were used for training. For instance, intervals S2 (22–43) and S2 (53–88) from scenario 2 containing only separated targets.

It is interesting to notice the "specialization" effect appearing when the rules obtained for each scenario obtain better results than those generated from other ones (although with different data sets than training), but worse in the rest. The rows "representative 1" and "representative 2" are from data samples containing a sample of conflictive situations in scenarios 1 and 2, with overlap, occlusions, and splits. The training with a "sufficient" sample of different situations obtained the best results. Finally, the row "all" represents the result obtained with a random sampling for training and validation complementary sets, applying cross validation, very similar to the best result. In fact, both sets resulted in sets of rules very similar to the one generated with all available data.

6. CONCLUSIONS AND FUTURE WORK

Fuzzy reasoning has been successfully applied to effectively solve the core problem of data association for video tracking under complex, high-density conditions. Specific domain knowledge is represented as a set of rules to adapt association decisions as a function of several heuristics inferred from experimentation. This approach allowed a robust and flexible design to cope with different situations and at the same time guarantee real-time operation with an efficient computation load, avoiding combinatorial enumeration as in other approaches. Results obtained in representative ground operations illustrate the system capabilities to solve complex scenarios and improve tracking accuracy, with a satisfactory trade-off between system performance and computation efficiency. Future works will extend evaluation on more samples and make use of ground truth data. Finally, an automatic procedure, based on neuro-fuzzy techniques, has been applied in order to obtain a set of rules from representative examples showing that the domain is susceptible to apply machine-learning techniques to tune its design, in this case, to refine the rules to decide the appropriate associations. The evaluation assessed the capability to decide the appropriate labels for each blob. A thorough evaluation with ground truth will measure the capability of learning processes to improve the accuracy and continuity performance of a given design of tracker, and this is also left for future work.

ACKNOWLEDGMENT

This work is funded by the Spanish CICYT (TIC2002-04491-C02-02).

REFERENCES

[1] G. Appenzeller and J. L. Crowley, "Experimental performance characterization of adaptive filters," in *Proc. IEEE 13th International Conference on Pattern Recognition (ICPR '96)*, vol. 2, pp. 417–421, Vienna, Austria, August 1996.

[2] H. R. Berenji and P. Khedkar, "Learning and tuning fuzzy logic controllers through reinforcements," *IEEE Trans. Neural Networks*, vol. 3, no. 5, pp. 724–740, 1992.

[3] J. A. Besada, J. Portillo, J. García, and J. M. Molina, "Image-Based automatic surveillance for airport surface," in *Proc. 4th International Conference on Information Fusion (FUSION '01)*, pp. 11–18, Montreal, Quebec, Canada, August 2001.

[4] J. Black, T. Ellis, and P. L. Rosin, "A novel method for video tracking performance evaluation," in *Proc. Joint IEEE International Workshop on Visual Surveillance and Performance Evaluation of Tracking and Surveillance (VS-PETS '03)*, pp. 125–132, Nice, France, October 2003.

[5] S. Blackman and R. Popoli, *Design and Analysis of Modern Tracking Systems*, Artech House, Norwood, Mass, USA, 1999.

[6] J. J. Buckley and Y. Hayashi, "Neural nets for fuzzy systems," *Fuzzy Sets and Systems*, vol. 71, no. 3, pp. 265–276, 1995.

[7] F. Dellaert, S. M. Seitz, C. E. Thorpe, and S. Thrun, "Structure from motion without correspondence," in *Proc. IEEE Conference on Computer Vision and Pattern Recognition (CVPR '00)*, vol. 2, pp. 557–564, Hilton Head Island, SC, USA, June 2000.

[8] A. P. Dempster, N. M. Laird, and D. B. Rubin, "Maximum likelihood from incomplete data via the EM algorithm," *Journal of the Royal Statistical Society B*, vol. 39, no. 1, pp. 1–38, 1977.

[9] Z. Ding, H. Leung, and L. Hong, "Decoupling joint probabilistic data association algorithm for multiple target tracking," *IEE Proceedings Radar, Sonar and Navigation*, vol. 146, no. 5, pp. 251–254, 1999.

[10] U.S. Department of Transportation. FAA, *The Future Airport Surface Movement Safety, Guidance and Control Systems: A Vision for Transition into the 21st Century*, Washington, USA, November 1993.

[11] J. García, J. A. Besada, J. M. Molina, J. Portillo, and G. de Miguel, "Fuzzy data association for image-based tracking in dense scenarios," in *Proc. IEEE International Conference on Fuzzy Systems (FUZZ-IEEE '02)*, vol. 2, pp. 902–907, Honolulu, Hawaii, USA, May 2002.

[12] H. Gauvrit, J. P. Le Cadre, and C. Jauffret, "A formulation of multitarget tracking as an incomplete data problem," *IEEE Trans. on Aerospace and Electronics Systems*, vol. 33, no. 4, pp. 1242–1257, 1997.

[13] M. Haag and H.-H. Nagel, "Tracking of complex driving manoeuvres in traffic image sequences," *Image and Vision Computing*, vol. 16, no. 8, pp. 517–527, 1998.

[14] S. K. Halgamuge and M. Glesner, "Neural networks in designing fuzzy systems for real world applications," *Fuzzy Sets and Systems*, vol. 65, no. 1, pp. 1–12, 1994.

[15] J.-S. R. Jang, "ANFIS: adaptive-network-based fuzzy inference systems," *IEEE Trans. Syst., Man, Cybern.*, vol. 23, no. 3, pp. 665–685, 1993.

[16] D. Koller, K. Daniilidis, and H.-H. Nagel, "Model-based object tracking in monocular image sequences of road traffic scenes," *International Journal of Computer Vision*, vol. 10, no. 3, pp. 257–281, 1993.

[17] E. H. Mamdani and J. Efstathion, "An analysis of formal logics as inference mechanism on expert systems," *International Journal of Man-Machine Studies*, vol. 21, no. 3, pp. 213–227, 1984.

[18] V. Matellán, C. Fernández, and J. M. Molina, "Genetic learning of fuzzy reactive controllers," *Robotics and Autonomous Systems*, vol. 25, no. 1-2, pp. 33–41, 1998.

[19] J. M. Mendel, "Fuzzy logic systems for engineering: a tutorial," *Proc. IEEE*, vol. 83, no. 3, pp. 345–377, 1995.

[20] D. Nauck and R. Kruse, "NEFCLASS—a neuro-fuzzy approach for the clasification of data," in *Proc. ACM Symposium on Applied Computing*, pp. 461–465, Nashville, Tenn, USA, February 1995.

[21] D. Nauck, R. Kruse, and R. Stellmach, "New learning algorithms for the neuro-fuzzy environment NEFCON-1," in *Proc. Neuro-Fuzzy Systems*, pp. 357–364, Darmstadt, Germany, 1995.

[22] D. Nauck, "Neuro-fuzzy systems: review and prospects," in *Proc. 5th European Congress on Intelligent Techniques and Soft Computing (EUFIT '97)*, pp. 1044–1053, Aachen, Germany, September 1997.

[23] J. H. Piater and J. L. Crowley, "Multi-modal tracking of interacting targets using Gaussian approximations," in *Proc. IEEE 2nd International Workshop on Performance Evaluation of Tracking and Surveillance (PETS '01)*, Kauai, Hawaii, USA, December 2001.

[24] D. Pokrajac and L. J. Latecki, "Spatiotemporal blocks-based moving objects identification and tracking," in *Proc. Joint IEEE International Workshop on Visual Surveillance and Performance Evaluation of Tracking and Surveillance (VS-PETS '03)*, Nice, France, October 2003.

[25] P. L. Rosin and E. Ioannidis, "Evaluation of global image thresholding for change detection," *Pattern Recognition Letters*, vol. 24, no. 14, pp. 2345–2356, 2003.

[26] M. Sugeno, "An introductory survey of fuzzy control," *Information Science*, vol. 36, no. 1-2, pp. 59–83, 1985.

[27] N. Tschichold-Gürman, "Generation and improvement of fuzzy classifier with incremental learning using fuzzy rulenet," in *Proc. ACM Symposium on Applied Computing*, pp. 466–470, Nashville, Tenn, USA, February 1995.

[28] L. A. Zadeh, "Outline of a new approach to the analysis of complex systems and decision processes," *IEEE Trans. Syst., Man, Cybern.*, vol. 3, no. 1, pp. 28–44, 1973.

[29] H. J. Zimmermann, *Fuzzy Set Theory and Its Applications*, Kluwer Academic, Norwell, Mass, USA, 1990.

Jesús García is currently an Associate Lecturer in the Computer Science Department, Universidad Carlos III de Madrid, since the year 2000. He received a degree in telecommunication engineering from Universidad Politécnica de Madrid in 1996, and the Ph.D. degree from the same university in 2001. He currently works in the Research Group of Applied Artificial Intelligence. Prior to this appointment, he had worked in the Data Processing and Simulation Group, Universidad Politécnica de Madrid. He has participated in several national and European projects related to air traffic management. His main interests are in artificial intelligence applied to engineering aspects in the context of radar and image data processing, navigation, and air traffic management. He is the author of more than 10 publications in journals and 30 publications in international conferences.

José M. Molina is an Associate Professor at the Universidad Carlos III de Madrid. He joined the Computer Science Department, Universidad Carlos III de Madrid in 1993. Currently he coordinates the Applied Artificial Intelligence Group (GIAA). His current research focuses on the application of soft computing techniques (NN, evolutionary computation, fuzzy logic, and multiagent systems) to radar data processing, air traffic management, and e-commerce. He is author of up to 20 journal papers and 80 conference papers. He received a degree in telecommunication engineering from the Universidad Politécnica de Madrid in 1993 and a Ph.D. degree from the same university in 1997.

Juan A. Besada received a degree in telecommunication engineering from the Universidad Politécnica de Madrid in 1996 and a Ph.D. degree from the same university in 2001. He has worked in the Signal Processing and Simulation Group of the same university since 1995, participating in several national and European projects related to air traffic control. He is currently an Associate Professor at Universidad Politécnica de Madrid. His main interests are air traffic control, navigation, and data fusion.

Javier I. Portillo received his B.S. and Ph.D. degrees in telecommunication engineering in 1985 and 1991, respectively, both from Universidad Politécnica de Madrid. Currently, he is a Professor in the Signal, System, and Radiocommunications Department, Telecommunication Engineering School, Universidad Politécnica de Madrid. His research interests are image processing, computer vision, and simulation, and the application of the preceding techniques to air traffic control. He is author or coauthor of many research papers and technical reports and he has worked in or managed more than 30 research public projects and private projects with enterprises.